

Quadruped Guidance Robot for the Visually Impaired: A Comfort-Based Approach

Yanbo Chen[†], Zhengzhe Xu[†], Zhuozhu Jian[†], Gengpan Tang, Yunong Yangli,
Anxing Xiao*, Xueqian Wang*, Bin Liang

Abstract—A quadrupedal guidance robot that can guide people and avoid various obstacles, could potentially be owned by more visually impaired people at a fairly low cost. Most of the previous guiding systems treat the robot as the majority without fully considering the human response behavior and comfort, and the human is more like an appendage being dragged by the robot. This may lead to less accurate guiding of the human and the force experienced by the human may also undergo large changes. In this paper, we propose a novel guidance robot system with a comfort-based concept. We design a leash containing an elastic rope and a thin string, and use a motor to adjust the length of the string to ensure comfort. We use the force-based human motion model to plan the forces experienced by the human. Afterward, the direction and magnitude of the force are controlled by the motion of the robot, and the rotation of the motor, respectively. This allows humans to be guided safely and more comfortably to the target position in complex environments. The system has been deployed on Unitree Laikago quadrupedal platform and validated in real-world scenarios. (Video¹)

I. INTRODUCTION

Guide dogs can lead the visually impaired to avoid obstacles, assist them to complete their daily activities and improve their quality of life. However, the number of guide dogs is extremely limited due to the high cost of time and money in training. In recent years, quadruped robots display the ability to achieve challenging dynamic motions, such as jumping over obstacles [1], and navigating in uneven terrain [2]. Quadruped robots also have extremely high reproducibility when their athletic ability is no less than that of real dogs, enabling more visually impaired to use guide dogs. In previous studies, whether the human and the robot were connected by a rigid arm [3]–[6] or a leash [7], they considered the robot to be the majority and the human to be an appendage at the rear of the robot. With this guiding method, human comfort is not taken into account, resulting



Fig. 1: A blind-folded person is guided by Unitree Laikago to turn out and cross the corridor. Human and robot are connected by a special leash, and a force control device is used to control the magnitude of force on the leash to ensure accuracy and comfort.

in a large variation in the traction force. Our goal in this paper is to propose a comfort-based quadruped guidance robot approach that can lead the human to a certain place in a complex indoor environment. First, we use a leash containing an elastic rope and a thin string to connect the human and the robot. Then, a force-based human motion model is established and used in the human motion planner to obtain forces that can guide human to the target position safely, efficiently and comfortably. Robot motion planning is used to ensure that the direction of the force is matched to the human motion planner. The force control device containing a motor is used to control the magnitude of the force, which allows for more precise control of human movement and ensures human comfort. Therefore, we utilize the quadruped robot Unitree Laikago to accomplish this task, guiding a blind-folded person to the target position with the special leash, as shown in Fig. 1.

A. Related Work

Guidance assistive technologies capable of guiding the visually impaired are a long-term study. As early as 1981, the guide dog robot MELDOG [8] realized the interaction between human and robot successfully through experimental hardware. In the beginning, guiding human was implemented mostly with wheeled robots as the mobile platform [9]–[11], which had limitations in complex terrain. With the development of robotic mobile platforms, footed robots [7], [12] and drones [13], [14] are also used as guiding humans

[†] indicates equal contribution.

* Corresponding authors: Anxing Xiao, Xueqian Wang.

This work is supported by Joint Funds of the National Natural Science Foundation of China U1813216.

Yanbo Chen, Zhengzhe Xu, Gengpan Tang, and Yunong Yangli are with the School of Mechanical Engineering and Automation at Harbin Institute of Technology, Shenzhen 518055, China, {190320129, 200320314, 190310113, 190320329}@stu.hit.edu.cn

Zhuozhu Jian, Xueqian Wang, and Bin Liang are with the Center for Artificial Intelligence and Robotics, Shenzhen International Graduate School, Tsinghua University, Shenzhen 518055, China, {jzz21@mails., wang.xq@sz., liangbin@tsinghua.edu.cn

Anxing Xiao is with Department of Electronic and Electrical Engineering at Southern University of Science and Technology, Shenzhen 518055, China, xiaox@mail.sustech.edu.cn

¹Video demonstration: <https://youtu.be/Xroov-UASC0>.

with more flexible movements and the potential to work in complex environments. However, the latter has weak load capacity that leads to limited installation of sensor modules.

Guiding the human is a complicated human-robot interaction task. The interaction methods, including haptic feedback-based guidance [15] and auditory guidance [16], [17], as well as traction. However, the haptic feedback-based approaches are difficult to ensure comfort and safety; auditory-based implementations are susceptible to interference from external noise, and the guidance may be inaccurate and unsafe. Therefore, more studies are now based on traction-based guidance. Traction guidance approaches, including the use of rigid connections [3], [4], [18] or flexible connections [7], [13] between a human and a robot. The rigid connection may result in a large and sudden change in the force on the human when walking or stopping suddenly. Using a leash connection is more flexible, [7] considers a hybrid system model that includes slack and tautness of the leash, but suffers from a long planning time and does not take into account the discomfort caused by multiple sudden changes in the traction force when it is repeatedly changed from slack to taut. As a result, previous work has focused more on the planning of the robot's path and lacked considerations based on the comfort and accuracy of the human being guided. We aim to establish a guidance robot system with a comfort-based concept.

B. Contributions

This work offers the following contributions:

- 1) A highly portable guide sensor platform, a leash containing elastic rope and thin string and a force control device are designed. The special leash and force control devices allow for more precise control of human movement while making human more comfortable.
- 2) A force-based human motion model to describe human behavior is proposed and used for motion planning. A human motion planner and a robot motion planner are proposed to ensure human comfort, where the force is used as a bridge.
- 3) The hardware platform and the system were deployed on the Unitree Laikago quadruped platform and validated in the experiment with real-world scenarios.

II. SYSTEM DESIGN

A. Mechanical System

The quadruped guidance robot, shown in Fig. 2, is 0.65m in length, 0.35m in width and 0.9m in height. It consists of three parts:

1) *Robotic Platform*: Unitree Laikago is a quadruped robotic platform, with a length of 0.65m, a width of 0.35m, a height of 0.6m, a maximum load of 5kg and a walking speed of $-0.5\sim 0.8\text{m/s}$. Due to the large size and strong load capacity of the robot dog, more equipment and more complex mechanisms can be loaded.

2) *Sensors*: A 2D LiDAR is mounted on the robot for perception and localization. An RGB-D camera is mounted on the 1-DoF gimbal to detect the human's position.

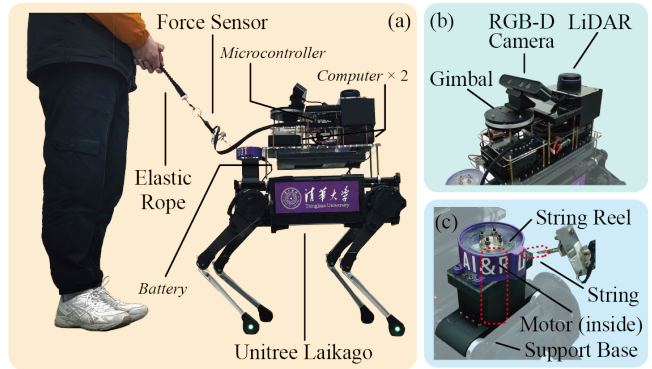


Fig. 2: The quadruped guidance robot consists of the quadruped platform (Fig. 2(a)), the sensors module (Fig. 2(b)), and the force control device module (Fig. 2(c)). In addition, high-performance computers and a high-capacity battery are equipped to support stable operation (Fig. 2(a)).

3) *Force Control Device*: The force control device is mounted at the rear of the robot. It consists of support base, DC gear motor, acrylic string reel, high-strength string, leash containing elastic rope and thin string, motor controller Arduino MEGA2560 with the PID control program uploaded. According to Hooke's Law $F = K\Delta l$, where K is the stiffness coefficient and Δl is the elongation, the magnitude of the force depends on the length of the elastic rope. When the distance between the human and robot remains unchanged, the length of the leash, that is, the total length of the elastic rope and the thin string, is fixed. The rotation of the motor can retract or release the string. Therefore, the length of the elastic rope can be adjusted by the rotation of the motor. Since the speed of retracting and releasing the string is much higher than the relative speed between human and robot, it can be assumed that the change of elastic rope's length in any short time depends on the motor speed, that is, motor speed determines the change in magnitude of force. The micro controller unit controls the motor, forming a closed loop with the force sensor. Thus, the force can be maintained at a certain magnitude by the rotation of the motor.

B. System Framework

As shown in Fig. 3, the guiding system can be divided into four modules: mapping and localization system, state estimation, planning system and control system.

In the mapping and localization system, the LiDAR is used for mapping and robot localization. LiDAR, gimbal, and RGB-D camera jointly measure the human position. In order to reduce the error and ensure better performance of the guiding system, each observed value and predicted value will be subjected to Unscented Kalman Filter, as detailed in III-D.

The grid map, point cloud and estimated state are passed into the planning system. The planning system is divided into path planning and motion planning. The path planner will search in the way in III-E, and obtain a collision-free human trajectory and pass it to the motion planner. In motion planning, we take into account that the human step and the robot and motor control have different frequencies:

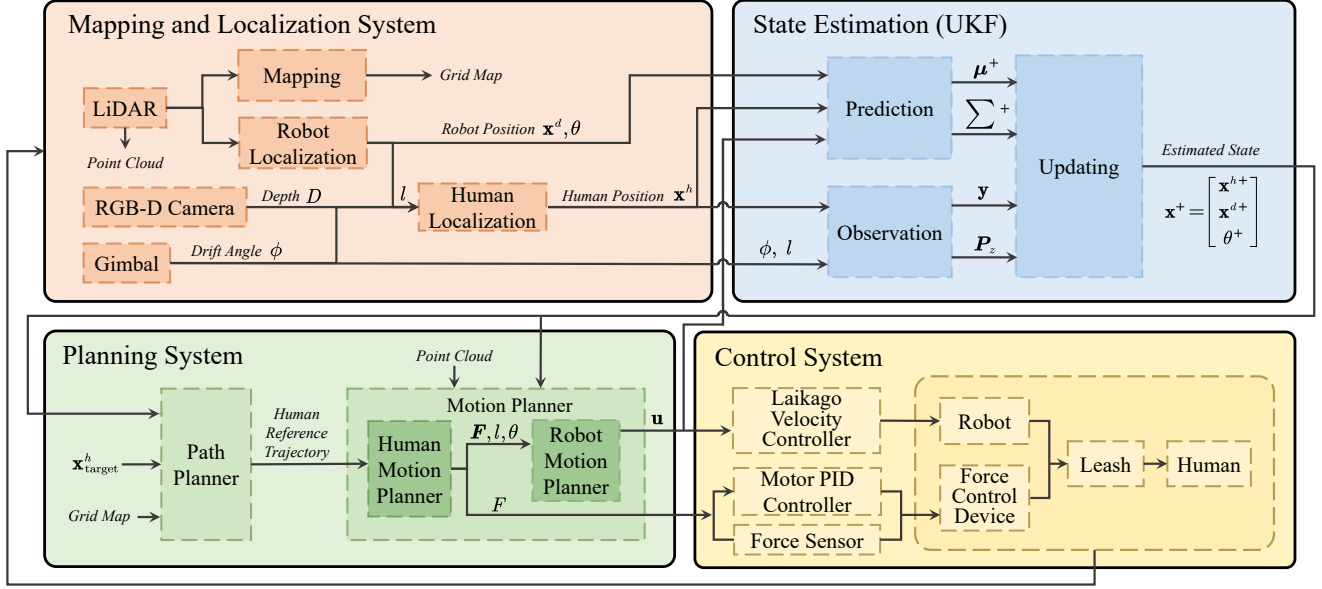


Fig. 3: Overview of system framework. The mapping and localization system obtains the system state. After state estimation (UKF), the estimated state is passed to the planner. The planner uses the grid map and state estimates to solve for the reference force and control inputs to the controllers.

the human step takes 0.4~0.7s, which is at a relatively low frequency, while the robot velocity and motor rotation can both be controlled at a high frequency. Thus, we separate human motion planning from robot motion planning. The required forces (magnitude and direction) are computed in the human motion planning described in III-C. At the same time, the robot motion planning is performed in a separate thread based on MPC to control the force direction, while the motor controller performs high-frequency PID control of the force magnitude. Finally, the human moves along the desired trajectory under the traction of the leash controlled by the robot and the force control device.

III. METHOD

A. System State Formulation

The human-robot guiding system consists of a human and a quadruped guidance robot connected by a leash, as shown in Fig. 4(a). System state is defined as $\mathbf{x} = [\mathbf{x}^h \ \mathbf{x}^d \ \theta]^\top \in \mathbb{R}^5$ in the world frame, where $\mathbf{x}^h = [x^h \ y^h]^\top$ and $\mathbf{x}^d = [x^d \ y^d]^\top$ are the position of human and robot respectively, and θ is the yaw angle of the robot. In addition, several feature points are set on the robot. As shown in Fig. 4(b), $\mathbf{x}^f = \mathbf{x}^d - d_{cf}\mathbf{e}_\theta$ is the leash fixing point, where d_{cf} is the distance between the fixed point of the leash and the center of the robot. Furthermore, \mathbf{x}^{dc_1} , \mathbf{x}^{dc_2} are the centers of the expansion circles for the robot's obstacle avoidance, and the leash is denoted as $\mathbf{l} = \mathbf{x}^f - \mathbf{x}^h = l\mathbf{e}_l \in \mathbb{R}^2$.

B. Force-Based Human Motion Model for Guiding System

In the guiding system, benefiting from the free movement of the robot and the flexible adjustment of the string length, we give priority to ensuring a safe walking path for the human and a more comfortable force when guiding. Therefore, we do not pay attention to the kinematics of the robot first,

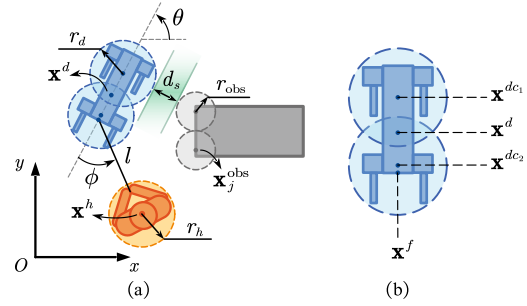


Fig. 4: Configuration of the guiding system. Human is guided by leash attached to the robot rear point \mathbf{x}^f (Fig. 4(a)). System can be described by $(x^h, y^h, x^d, y^d, \theta)$. The four feature points \mathbf{x}^d , \mathbf{x}^f , \mathbf{x}^{dc_1} , \mathbf{x}^{dc_2} are set on the robot (Fig. 4(b)).

but consider the movement trend of a human under a certain magnitude and direction of force during walking. The force $\mathbf{F} = F\mathbf{e}_F \in \mathbb{R}^2$ acting on the person is the focus of the analysis of human motion. Obviously, the force is in the same direction as the leash, i.e., $\mathbf{e}_F = \mathbf{e}_l$.

Human walking is a discrete process, which can be written as $\mathbf{x}_{k+1}^h = \mathbf{x}_k^h + \mathbf{s}_k$, where \mathbf{s}_k represents one step. The size and direction of the step are related to the relative position of the robot and the human as well as the magnitude of the force acting on the human. We take the ratio of the average step size \bar{s} to the time interval T , which is considered to be the velocity of human: $\mathbf{v}^h = \bar{s}/T$. Therefore, human's state equation can be written as $\mathbf{x}_{k+1}^h = \mathbf{x}_k^h + \mathbf{v}_k^h T$. During the guiding process, human motion can be divided into two states: standing and walking, denoted as q_s and q_w , respectively. Human movement depends on the force on the leash and human's current state.

1) *Standing State*: When the human is standing still, we have $\mathbf{v}^h = \mathbf{0}$. The position of the robot can be determined

by the leash length and the yaw angle as shown in Fig. 4:

$$\mathbf{x}^d = \mathbf{f}_d(\mathbf{x}^h, \mathbf{F}, l, \theta) = \mathbf{x}^h + l\mathbf{e}_F + d_{cf}\mathbf{e}_\theta. \quad (1)$$

2) *Walking State*: When the human is walking, the movement direction tends to the direction of the force. The step size is related to the magnitude of the force applied. The experiment in IV-A illustrates the relationship between the velocity of the human moving along the leash direction and the force as

$$\mathbf{v}^{hl} = \mathbf{v}^h \cdot \mathbf{e}_l = \alpha F + \beta \quad (2)$$

where the coefficient $\alpha, \beta \in \mathbb{R}$ takes different values for different individuals. The position of the robot still can be computed by (1).

3) *State Transfer Condition*: A human switches from standing to walking depending on the rate of change of the applied force. According to the minimum-jerk theory [19], when a sudden change in force is acted on to the human's arm, human tends to minimize the rate of change of acceleration (jerk). Therefore, the human starts to walk in the force direction. When human is walking, the magnitude of the force needs to be greater than a certain threshold F_{th} , so that human can maintain walking. Otherwise, human will stop. We introduce a state machine to describe the state transition condition between two states, as shown in Fig. 5.

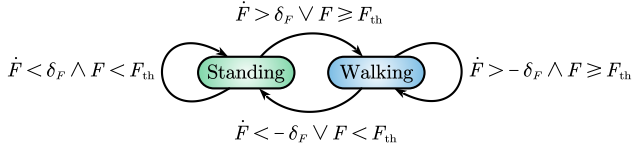


Fig. 5: Two motion states of a guided human: standing and walking. The state transition is related to the current state of the human and the force.

We define $q_s = 0$, $q_w = 1$, and the rate of change of the force $\Delta F_k = F_{k+1} - F_k$. The discrete-time state transfer equation is formulated as

$$q_{k+1} = \delta(q_k, F_{k+1}, F_k) = \begin{cases} 0, & \text{if } (q_k = 0 \wedge (\Delta F_k < \delta_F \cdot T \wedge F_k < F_{th})) \\ & \vee (q_k = 1 \wedge (\Delta F_k < -\delta_F \cdot T \vee F_k < F_{th})) \\ 1, & \text{if } (q_k = 0 \wedge (\Delta F_k > \delta_F \cdot T \vee F_k \geq F_{th})) \\ & \vee (q_k = 1 \wedge (\Delta F_k > -\delta_F \cdot T \wedge F_k \geq F_{th})) \end{cases}. \quad (3)$$

Therefore, the state equation for human based on the human motion state machine model is formulated as

$$\mathbf{x}_{k+1}^h = \mathbf{f}_h(\mathbf{x}_k^h, \mathbf{F}_k, q_k) = \mathbf{x}_k^h + q_k \mathbf{v}_k^{hl} \mathbf{e}_{F_k} T. \quad (4)$$

In this model, the parameters $\{\alpha, \beta, \delta_F, F_{th}\}$ have different values for different individuals. The parameter adaptation methods are described in IV-A.

C. Motion Planning

The motion planning is the key to ensuring that a person walks safely with comfortable force traction. In our guiding system, the human motion and the robot motion are planned

in two stages. In the first stage, the human motion planner will be performed using the force-based human motion model to obtain a reference force and pass it to the force control device. In addition, the forces and leash lengths and yaw angles derived in the first stage are passed into the robot motion planner to derive the robot control inputs by applying MPC-based trajectory tracking. In this way, the robot can reach the appropriate position to control the force direction.

1) *Human Motion Planning*: The force-based human motion model is used to plan for the magnitude and direction of the force that can guide the human comfortably along a reference path. Since the relative position of the robot and human determines the direction of the force, and the robot's obstacle avoidance is a strong constraint, the robot's position needs to be considered as a constraint in the planning. Since the specific position of the robot can be computed by (1), the optimization variables in the human motion planning are set to $\{\mathbf{F}, l, \theta\}$. To achieve the force planning task, we achieve optimal control by formulating the following MPC problem with a horizon of N steps:

$$\begin{aligned} \min_{\{\mathbf{F}_k, l_k, \theta_k\}} & \|\mathbf{x}_N^h - \mathbf{x}_{\text{target}}^h\|_{\mathbf{Q}_t^h} + \sum_{k=0}^{N-1} (\|\mathbf{x}_k^h - \mathbf{x}_k^{h*}\|_{\mathbf{Q}^h} \\ & + \|\mathbf{F}_{k+1} - \mathbf{F}_k\|_{\mathbf{Q}_F} + w_{\Delta\theta} (1 - \cos(\theta_{k+1} - \theta_k)) \\ & + w_l (K(l_{k+1} - l_k) + (F_{k+1} - F_k)))^2 \end{aligned} \quad (5a)$$

$$\text{s.t. } \mathbf{x}_0 = \mathbf{x}_{\text{curr}}, \quad q_0 = q_{\text{curr}} \quad (5b)$$

$$\mathbf{x}_{k+1}^h = \mathbf{f}_h(\mathbf{x}_k^h, \mathbf{F}_k, q_k) \quad (5c)$$

$$\mathbf{x}_{k+1}^d = \mathbf{f}_d(\mathbf{x}_{k+1}^h, \mathbf{F}_k, l_k, \theta_k) \quad (5d)$$

$$q_{k+1} = \delta(q_k, F_{k+1}, F_k) \quad (5e)$$

$$F_{\min} \leq \|\mathbf{F}_k\| \leq F_{\max} \quad (5f)$$

$$l_{\min} \leq l_k \leq l_{\max} \quad (5g)$$

$$\langle \mathbf{e}_{F_{k+1}}, \mathbf{e}_{F_k} \rangle \geq \cos(\varphi_F) \quad (5h)$$

$$\langle \mathbf{e}_{F_k}, \mathbf{e}_{\theta_k} \rangle \geq \cos(\varphi_\theta) \quad (5i)$$

$$\|\mathbf{x}_k^h - \mathbf{x}_j^{\text{obs}}\| \geq d_s + r_h + r_{\text{obs}} \quad (5j)$$

$$\|\mathbf{x}_k^{dc_i} - \mathbf{x}_j^{\text{obs}}\| \geq d_s + r_d + r_{\text{obs}} \quad (i = 1, 2) \quad (5k)$$

where $\|\mathbf{x}\|_{\mathbf{Q}} := \frac{1}{2} \mathbf{x}^\top \mathbf{Q} \mathbf{x}$. \mathbf{Q}_t^h , \mathbf{Q}^h , $\mathbf{Q}_F \in \mathbb{R}^{2 \times 2}$ are positive definite, w_l , $w_{\Delta\theta}$, $w_{\theta_0} \in \mathbb{R}$ are weight coefficients. \mathbf{x}_k^{h*} ($k = 0, 1, \dots, N$) are the collision-free human waypoints passed in by path planning, d_s is the safety distance, r_h, r_d, r_{obs} are the expansion radii of human, robot and obstacle, respectively. φ_F is the upper bound of the direction mutation of the force, and φ_θ is the upper bound of the difference between the robot's yaw angle and the directional angle of force.

In the cost function, $\|\mathbf{x}_k^h - \mathbf{x}_k^{h*}\|_{\mathbf{Q}^h}$ ensures that the human trajectory fits the reference path and $\|\mathbf{x}_N^h - \mathbf{x}_{\text{target}}^h\|_{\mathbf{Q}_t^h}$ is the terminal cost. The term $\|\mathbf{F}_{k+1} - \mathbf{F}_k\|_{\mathbf{Q}_F}$ minimizes the changes in forces, so that force can change smoothly to ensure comfort. The term $w_{\Delta\theta} (1 - \cos(\theta_{k+1} - \theta_k))$ minimizes the changes in yaw angle, which implies kinematic constraints. Further more, $w_l (K(l_{k+1} - l_k) + (F_{k+1} - F_k))^2$ ensures that force

changes are provided as far as possible by the deformation of the elastic rope, minimizing motor rotation.

In the constraints, the force-based human motion model is used to compute the system state. In addition, the upper and lower bounds of force and the leash length, the change of the direction of force, the angle between yaw angle and the directional angle of force are constrained in (5f), (5g), (5h), (5i), respectively. We use one circle to cover the human and two circles to cover the robot as shown in Fig. 2(a) to avoid obstacles by (5j) and (5k).

2) *Robot Motion Planning*: The robot motion planning aims to obtain the control input to bring the robot to the position suitable for pulling the human. The reference quantities $\{\mathbf{F}_k^*, l_k^*, \theta_k^*\}$ obtained from human motion planning will be used in this stage. Knowing \mathbf{F}_k^* and the current state of the human, it is able to obtain the expected position and state of the human \mathbf{x}_k^{h*} and \mathbf{q}_k^{h*} by (3) and (4). \mathbf{x}_k^{d*} can be computed by (1) using l_k^* and θ_k^* . Moreover, the position of robot can be calculated by

$$\tilde{\mathbf{x}}_{k+1}^d = \tilde{\mathbf{x}}_k^d + \mathbf{R}_{z,k} \mathbf{u}_k T, \quad \text{if } q_k^* = q_s \quad (6)$$

$$\tilde{\mathbf{x}}_{k+1}^d = \tilde{\mathbf{x}}_k^d + \mathbf{D} \mathbf{R}_{z,k} \mathbf{u}_k T, \quad \text{if } q_k^* = q_w \quad (7)$$

where $\tilde{\mathbf{x}}^d = [x^d \ y^d \ \theta]^T$ is the generalized coordinates of robot and $\mathbf{u} = [v_x \ v_y \ \omega]^T$ is robot's control input. $\mathbf{D} \in \mathbb{R}^{3 \times 3}$ is the velocity discount coefficient matrix caused by being pulled, $\mathbf{R}_z \in \mathbb{R}^{3 \times 3}$ is the rotation matrix corresponding to the yaw angle. Based on an MPC problem with a horizon of M steps, we minimize the cost function

$$J(\mathbf{u}) = \sum_{k=0}^{M-1} \left(\|\tilde{\mathbf{x}}_k^d - \tilde{\mathbf{x}}_k^{d*}\|_{\mathbf{Q}^d} + \|\mathbf{u}_k\|_{\mathbf{R}^d} \right) \quad (8)$$

where $\mathbf{Q}^d, \mathbf{R}^d \in \mathbb{R}^{3 \times 3}$ are positive definite, and implement obstacle avoidance by (5j) and (5k) to ensure safety.

For accuracy and real-time, the time step of human motion planner and robot motion planner are set differently. The former has a longer time step with a lower frequency to match the human step frequency, while the latter has a higher frequency for closed-loop control of the robot's position. The problems are formulated in CasADi [20] and solved with IPOPT [21].

D. State Observation and Estimation

Knowing robot and human states online is critical for the guiding system. We use Cartographer [22] for real-time mapping and robot localization. Further, to obtain the position of the human, an RGB-D camera is used to detect and recognize the human's face through OpenCV DNN-based Face Detection and Recognition [23]. The camera is mounted on a 1-DoF gimbal with coordinates \mathbf{x}^d which can rotate and return its rotation angle. The gimbal ensures that the face is always in the center of the camera's field of view. We denote the average depth of facial feature points as D_f , the angle returned by gimbal as ϕ , and the horizontal distance between human and camera as l_c , which can be calculated by $l_c = D_f / \cos(\varphi) - (H - h_c) \tan(\varphi)$, where H is human's body height and φ, h_c are the camera's fixed inclination angle

and height, relatively. Therefore, the position of the human can be computed by $\mathbf{x}^h = \mathbf{x}^d - l_c \mathbf{e}_{\theta+\phi}$.

Since the guiding system is a relatively complex nonlinear system, the Unscented Kalman Filter (UKF) is used for state estimation in this experiment.

For each sigma point, the weight of the center point is $\omega_0 = k / (n + k)$, and the weight of the remaining points is $\omega_i = 1 / 2(n + k)$. In this way, given a set of sigma points and a state transfer function, a new mean and covariance transformed by the function can be calculated. When the human is walking, the system state can be computed by

$$\mathbf{x}^+ = \mathbf{x} + \left(\begin{bmatrix} \alpha \mathbf{I}_2 & \mathbf{0} \\ \mathbf{0} & \mathbf{D} \mathbf{R}_z \end{bmatrix} \begin{bmatrix} \mathbf{F} \\ \mathbf{u} \end{bmatrix} + \begin{bmatrix} \beta \mathbf{e}_F \\ \mathbf{0} \end{bmatrix} \right) T + \mathbf{w} \quad (9)$$

and when human is standing, the state is given by $\mathbf{x}^+ = \mathbf{x} + [\mathbf{0} \ \mathbf{R}_z \mathbf{u} T]^T + \mathbf{w}$, where \mathbf{x}^+ is the state of the system at the next moment. Denote the direction angle of force \mathbf{F} by θ^h , which represents the direction that the human is heading. \mathbf{w} is the disturbance at the input, which is a random variable whose covariance is the error matrix $\mathbf{Q}_e = \text{diag}(\mathbf{Q}_h, \mathbf{Q}_d)$ where $\mathbf{Q}_h = \text{diag}(\sigma_{F,x^h}^2, \sigma_{F,y^h}^2)$ and $\mathbf{Q}_d = \text{diag}(\sigma_x^2, \sigma_y^2, \sigma_\theta^2)$. In the equation, $\sigma_x^2, \sigma_y^2, \sigma_\theta^2$ are the variances of x, y, θ , respectively, which are the errors introduced by the modeling process of the system, exported by Cartographer. $\sigma_{F,x^h}^2, \sigma_{F,y^h}^2$ are the error introduced when fitting force \mathbf{F} and human velocity \mathbf{v}^h , obtained from experimental data.

For each measurement, transform sigma points into measurement space:

$$\begin{aligned} \hat{\mathbf{z}} &= [\hat{l} \ \hat{\phi} \ \hat{x}^d \ \hat{y}^d \ \hat{\theta}]^T \\ &= [l \ \theta_e - \theta \ x^d \ y^d \ \theta]^T + \mathbf{v} \end{aligned} \quad (10)$$

where \mathbf{v} is the error during measurement, which is random and introduced due to the accuracy of the sensors and the measurement method. $\mathbf{R} = \text{diag}(\sigma_l^2, \sigma_\phi^2, \sigma_{s,x}^2, \sigma_{s,y}^2, \sigma_{s,\theta}^2)$ is the covariance of \mathbf{v} , which is the observation error matrix of the system.

E. Path Planning

We use a heap-based A* planner over the grid map to generate a collision-free human waypoints set. Human's coordinate is extended to $\tilde{\mathbf{x}}^h = [x^h \ y^h \ \theta^h]^T \in \mathbb{R}^3$. The transition between nodes representing one step of human is defined as $(\Delta L, \Delta\theta^h)$, where $\Delta L = \sqrt{(\Delta x^h)^2 + (\Delta y^h)^2}$ represents human's step size and $\Delta\theta^h$ represents the difference in the direction angle of the step. By limiting the size of $\Delta\theta^h$, the direction of human movement can not be greatly changed. The node cost $g(\tilde{\mathbf{x}}_n^h) = \sum_{i=1}^n \|\tilde{\mathbf{x}}_i^h - \tilde{\mathbf{x}}_{i-1}^h\|_2$ and the heuristic cost $h(\tilde{\mathbf{x}}_n^h) = \|\tilde{\mathbf{x}}_n^h - \tilde{\mathbf{x}}_{\text{target}}^h\|_2$. We assume that human always move in the direction of force. Since $\mathbf{e}_F = \mathbf{e}_l$, robot's position can be calculated from θ^h and the leash's length. We use breadth-first search to determine whether there is a continuous collision free trajectory for the robot to go from \mathbf{x}_{n-1}^d to \mathbf{x}_n^d , in order to judge whether human can transfer from $\tilde{\mathbf{x}}_{n-1}^h$ to $\tilde{\mathbf{x}}_n^h$. The collision-free human waypoints set is passed to the motion planner.

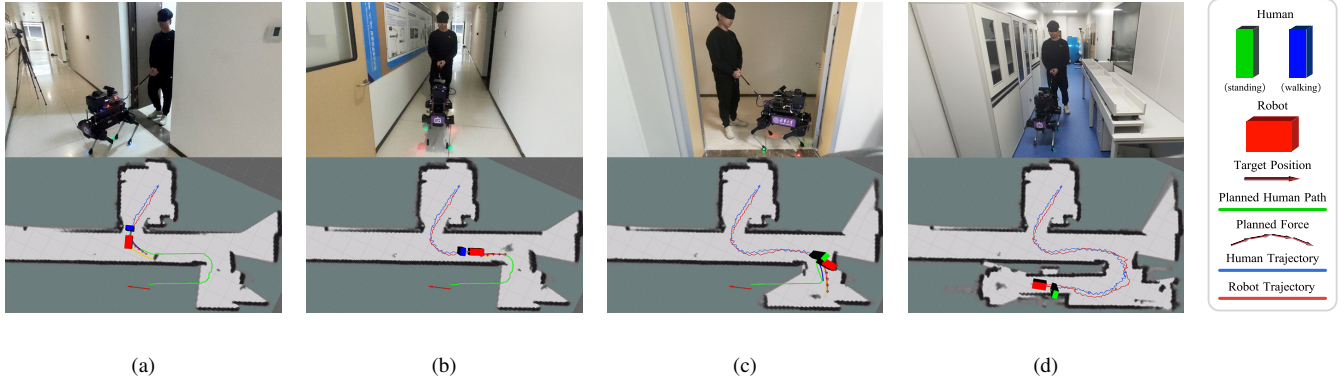


Fig. 7: Snapshots of the guiding process in a real-world scenario. Laikago guided a blind-folded person from the elevator lobby, through two doors and two corridors, to the target position in the laboratory.

IV. EXPERIMENTS

A. System Identification and Adaptive Parameter Estimation

Before establishing the human motion model, we have acquired experimental data from several subjects. It shows that the velocity of a human moving in the direction of the leash is positively correlated with the force experienced by humans. This relationship can be described by a linear function with slope α and intercept β , and with individual differences. Therefore, we designed an adaptive identification module to obtain the parameters in the $F-v^{hl}$ relationship of the first-time user of the system relatively quickly. To collect data, the module allows the robot to perform uniformly accelerated linear motion without force control devices enabled and guides the human forward. By measuring the actual velocity and force, after low-pass filtering to remove noise, the least-squares fitting is performed to obtain the model parameters.

Fig. 6 shows the different responses of different experimental objects to the force in the experiment of adaptive identification, as well as the adaptive results.

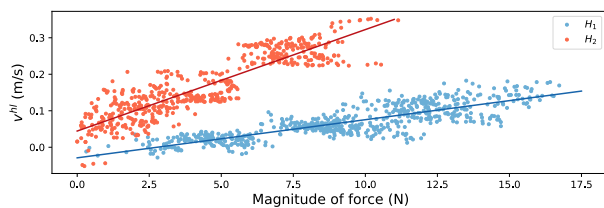


Fig. 6: $F-v^{hl}$ curves of two experimental subjects H_1, H_2 . The parameters of the linear fit are: $\alpha_1 = 0.0105$, $\beta_1 = -0.0290$; $\alpha_2 = 0.0278$, $\beta_2 = 0.0444$.

B. Robot Guiding Human Experiments

The experiments were conducted in a real-world scenario containing multiple test samples. In one set of tests, the robot guided a blind-folded person from the elevator lobby to a laboratory with a narrow corridor. As shown in Fig. 7, the door closer to the starting point is 1.1m in width, the other is 1.3m in width. The two corridor widths are 1.5m and 1m. Due to the long length of the system configuration,

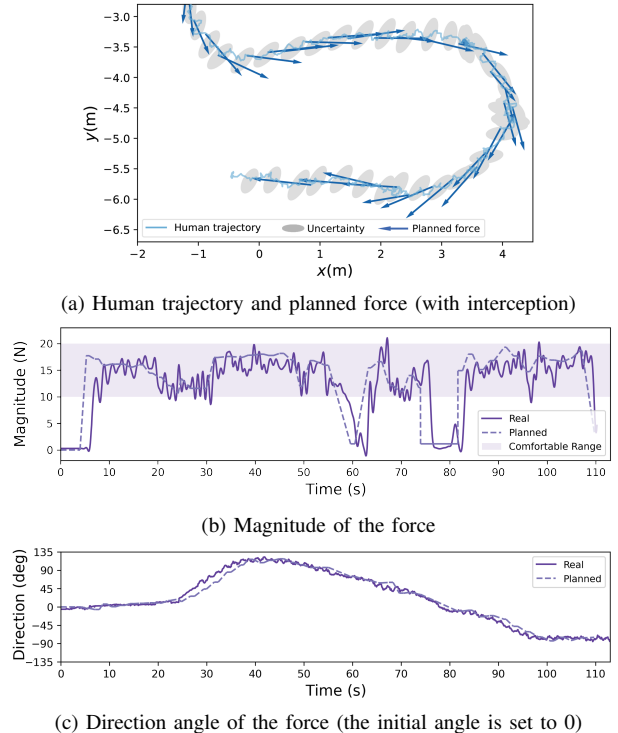


Fig. 8: Experimental results of the guiding process. (a) is the intercepted portion of the human trajectory (with 95% confidence interval) and the planned force. (b), (c) is the magnitude and direction of the planned force and the real force over time, respectively.

some accidents may occur when a rigid arm or a non-retractable leash is used to connect the human and the robot. For example, the robot may repeatedly adjust and try to pull the person through, which will keep the human in place for a large amount of time and reduce comfort. In contrast, our proposed comfort-based guiding system can ensure continuity and comfort when walking.

To obtain the real-time system state, we combine the information of observers with the state equation (9) to awaken nonlinear filtering, and the uncertainty in human location represented by covariance is visualized as a gray ellipse in Fig. 8(a). As the robot started to move, the observation data was continuously updated, the uncertainty of both human and

robot positions gradually decreased and stabilized.

As shown in Fig. 8(b), the experiment began with the motor rotating and shortening the string. At this time, people felt the change of force and began to walk.

When the person walked out of the first door, as shown in Fig. 7(a), the width of the door and the corridor was cleverly used to minimize the turning angle. During the process, the person did not slow down or stop. It can be seen that the human motion planner tends to ensure the continuity and comfort of human walking. When the person was about to enter the second door, as shown in Fig. 7(c), it was difficult to enter with the previous strategy because of the 180 degree corner. During 61~64s and 76~83s, as shown in Fig. 8(b), the force decreased rapidly and the human transformed to standstill after feeling it. In this case, the robot could move freely, the motor released the string to ensure that the force was maintained at a lower value. After the robot moved to the proper position, the string was shortened, and the human moved together with the robot. It can be seen that there was no repeated standing-walking switch that caused the person to feel uncomfortable.

Throughout the experiment, it can be concluded from Fig. 8(b) and 8(c) that the force planned on the basis of comfort ensures that the human path is as continuous as possible, minimizes the transfer of the walking-to-standing state, maintains a comfortable force magnitude, and a gentle and continuous pull without great changes in magnitude and direction.

V. CONCLUSION AND FUTURE WORK

Our work proposes a comfort-based quadruped guidance robot system, which is validated in experiments. A force-based human motion model, including standing and walking modes, is used in planning. The human motion planner solves for the magnitude and direction of the force. The robot motion planner solves for the control input, which ensures the direction of the force. The magnitude of the force is controlled by the force control device. The proposed approach was deployed and validated on Unitree Laikago to guide blind-folded people in narrow corridors. The experimental results indicate that the human motion planner can plan the forces experienced by the human, switch the mode, and guide the human to reach the target position safely and comfortably. Future work will focus on more complex applications in large-scale scenarios, such as cross-floor guidance task and safe sidewalk navigation.

REFERENCES

- [1] S. Gilroy, D. Lau, L. Yang, E. Izaguirre, K. Biermayer, A. Xiao, M. Sun, A. Agrawal, J. Zeng, Z. Li *et al.*, "Autonomous navigation for quadrupedal robots with optimized jumping through constrained obstacles," in *2021 IEEE 17th International Conference on Automation Science and Engineering (CASE)*. IEEE, 2021, pp. 2132–2139.
- [2] C. Mastalli, I. Havoutis, M. Focchi, D. G. Caldwell, and C. Semini, "Motion planning for quadrupedal locomotion: Coupled planning, terrain mapping, and whole-body control," *IEEE Transactions on Robotics*, vol. 36, no. 6, pp. 1635–1648, 2020.
- [3] J. Borenstein and I. Ulrich, "The guidecane—a computerized travel aid for the active guidance of blind pedestrians," in *Proceedings of International Conference on Robotics and Automation*, vol. 2. IEEE, 1997, pp. 1283–1288.
- [4] T.-K. Chuang, N.-C. Lin, J.-S. Chen, C.-H. Hung, Y.-W. Huang, C. Teng, H. Huang, L.-F. Yu, L. Giarré, and H.-C. Wang, "Deep trail-following robotic guide dog in pedestrian environments for people who are blind and visually impaired—learning from virtual and real worlds," in *2018 IEEE International Conference on Robotics and Automation (ICRA)*. IEEE, 2018, pp. 5849–5855.
- [5] Z. Li and R. Hollis, "Toward a ballbot for physically leading people: A human-centered approach," in *2019 IEEE/RSJ International Conference on Intelligent Robots and Systems (IROS)*. IEEE, 2019, pp. 4827–4833.
- [6] K. A. Hamed, V. R. Kamidi, W.-L. Ma, A. Leonessa, and A. D. Ames, "Hierarchical and safe motion control for cooperative locomotion of robotic guide dogs and humans: A hybrid systems approach," *IEEE Robotics and Automation Letters*, vol. 5, no. 1, pp. 56–63, 2019.
- [7] A. Xiao, W. Tong, L. Yang, J. Zeng, Z. Li, and K. Sreenath, "Robotic guide dog: Leading a human with leash-guided hybrid physical interaction," in *2021 IEEE International Conference on Robotics and Automation (ICRA)*. IEEE, 2021, pp. 11 470–11 476.
- [8] S. Tachi, K. Tanie, K. Komoriya, Y. Hosoda, and M. Abe, "Guide dog robot—its basic plan and some experiments with meldog mark i," *Mechanism and Machine Theory*, vol. 16, no. 1, pp. 21–29, 1981.
- [9] R. Soltani-Zarrin, A. Zeiaee, and S. Jayasuriya, "Pointwise angle minimization: A method for guiding wheeled robots based on constrained directions," in *Dynamic Systems and Control Conference*, vol. 46209. American Society of Mechanical Engineers, 2014, p. V003T48A004.
- [10] Y.-P. Hsu, C.-C. Tsai, Z.-C. Wang, Y.-J. Feng, and H.-H. Lin, "Hybrid navigation of a four-wheeled tour-guide robot," in *2009 ICCAS-SICE*. IEEE, 2009, pp. 4353–4358.
- [11] J. Guerreiro, D. Sato, S. Asakawa, H. Dong, K. M. Kitani, and C. Asakawa, "Cabot: Designing and evaluating an autonomous navigation robot for blind people," in *The 21st International ACM SIGACCESS conference on computers and accessibility*, 2019, pp. 68–82.
- [12] D. R. Bruno, M. H. de Assis, and F. S. Osório, "Development of a mobile robot: Robotic guide dog for aid of visual disabilities in urban environments," in *2019 Latin American Robotics Symposium (LARS), 2019 Brazilian Symposium on Robotics (SBR) and 2019 Workshop on Robotics in Education (WRE)*. IEEE, 2019, pp. 104–108.
- [13] E. Folmer, "Exploring the use of an aerial robot to guide blind runners," *ACM SIGACCESS accessibility and computing*, no. 112, pp. 3–7, 2015.
- [14] H. Tan, C. Chen, X. Luo, J. Zhang, C. Seibold, K. Yang, and R. Stiefelhagen, "Flying guide dog: Walkable path discovery for the visually impaired utilizing drones and transformer-based semantic segmentation," *arXiv preprint arXiv:2108.07007*, 2021.
- [15] R. K. Katzschmann, B. Araki, and D. Rus, "Safe local navigation for visually impaired users with a time-of-flight and haptic feedback device," *IEEE Transactions on Neural Systems and Rehabilitation Engineering*, vol. 26, no. 3, pp. 583–593, 2018.
- [16] S. Kalpana, S. Rajagopalan, R. Ranjith, and R. Gomathi, "Voice recognition based multi robot for blind people using lidar sensor," in *2020 International Conference on System, Computation, Automation and Networking (ICSCAN)*. IEEE, 2020, pp. 1–6.
- [17] L. Yang, I. Herzi, A. Zakhori, A. Hiremath, S. Bazargan, and R. Tames-Gadam, "Indoor query system for the visually impaired," in *International Conference on Computers Helping People with Special Needs*. Springer, 2020, pp. 517–525.
- [18] C. Ye, S. Hong, X. Qian, and W. Wu, "Co-robotic cane: A new robotic navigation aid for the visually impaired," *IEEE Systems, Man, and Cybernetics Magazine*, vol. 2, no. 2, pp. 33–42, 2016.
- [19] T. Flush, "The coordination of arm movements: an experimentally confirmed mathematical model," *J. neurosciences*, vol. 5, 1987.
- [20] J. A. Andersson, J. Gillis, G. Horn, J. B. Rawlings, and M. Diehl, "Casadi: a software framework for nonlinear optimization and optimal control," *Mathematical Programming Computation*, vol. 11, no. 1, pp. 1–36, 2019.
- [21] L. T. Biegler and V. M. Zavala, "Large-scale nonlinear programming using ipopt: An integrating framework for enterprise-wide dynamic optimization," *Computers and Chemical Engineering*, vol. 33, no. 3, pp. 575–582, 2009.
- [22] W. Hess, D. Kohler, H. Rapp, and D. Andor, "Real-time loop closure in 2d lidar slam," in *2016 IEEE International Conference on Robotics and Automation (ICRA)*, 2016, pp. 1271–1278.
- [23] G. Bradski and A. Kaehler, *Learning OpenCV: Computer vision with the OpenCV library*. O'Reilly Media, Inc., 2008.